



Title	Development of compartment for studies on the growth of protein crystals in space
Author(s)	Yamazaki, T.; Tsukamoto, K.; Yoshizaki, I.; Fukuyama, S.; Miura, H.; Shimaoka, T.; Maki, T.; Oshi, K.; Kimura, Y.
Citation	Review of Scientific Instruments, 87(3), 033107 https://doi.org/10.1063/1.4942961
Issue Date	2016-03-15
Doc URL	http://hdl.handle.net/2115/64701
Rights	This article may be downloaded for personal use only. Any other use requires prior permission of the author and AIP Publishing. The following article appeared in Review of Scientific Instruments 87, 033107 (2016); doi: 10.1063/1.4942961 and may be found at http://scitation.aip.org/content/aip/journal/rsi/87/3/10.1063/1.4942961 .
Type	article
File Information	1.4942961.pdf



[Instructions for use](#)

Development of compartment for studies on the growth of protein crystals in space

T. Yamazaki, K. Tsukamoto, I. Yoshizaki, S. Fukuyama, H. Miura, T. Shimaoka, T. Maki, K. Oshi, and Y. Kimura

Citation: [Review of Scientific Instruments](#) **87**, 033107 (2016); doi: 10.1063/1.4942961

View online: <http://dx.doi.org/10.1063/1.4942961>

View Table of Contents: <http://scitation.aip.org/content/aip/journal/rsi/87/3?ver=pdfcov>

Published by the [AIP Publishing](#)

Articles you may be interested in

[Modeling crystal growth from solution with molecular dynamics simulations: Approaches to transition rate constants](#)

J. Chem. Phys. **136**, 034704 (2012); 10.1063/1.3677371

[Molecular dynamics simulations of glycine crystal-solution interface](#)

J. Chem. Phys. **131**, 184705 (2009); 10.1063/1.3258650

[Interferometric Techniques for Investigating Growth and Dissolution of Crystals in Solutions](#)

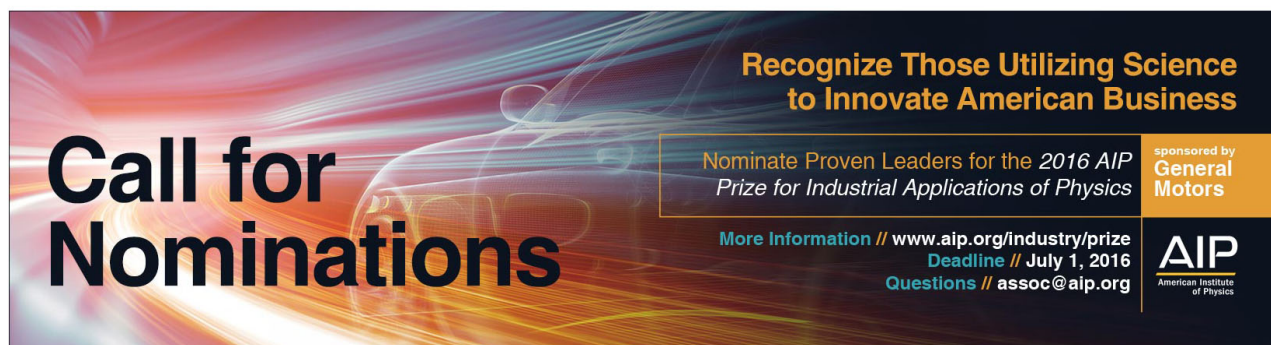
AIP Conf. Proc. **916**, 329 (2007); 10.1063/1.2751922

[Spherulitic growth kinetics of protein crystals](#)

Appl. Phys. Lett. **81**, 1975 (2002); 10.1063/1.1506208

[A statistical rate theory study of interface concentration during crystal growth or dissolution](#)

J. Chem. Phys. **108**, 8698 (1998); 10.1063/1.476298



Call for Nominations

Recognize Those Utilizing Science to Innovate American Business

Nominate Proven Leaders for the *2016 AIP Prize for Industrial Applications of Physics*

More Information // www.aip.org/industry/prize
Deadline // July 1, 2016
Questions // assoc@aip.org

sponsored by
General Motors

AIP
American Institute of Physics

Development of compartment for studies on the growth of protein crystals in space

T. Yamazaki,^{1,2,a)} K. Tsukamoto,^{1,3} I. Yoshizaki,⁴ S. Fukuyama,⁵ H. Miura,⁶ T. Shimaoka,⁷ T. Maki,⁸ K. Oshi,¹ and Y. Kimura²

¹Department of Earth Science, Graduate School of Science, Tohoku University, 6-3 Aramaki Aza Aoba, Aoba-ku, Sendai, Miyagi 980-8578, Japan

²Institute of Low Temperature Science, Hokkaido University, Kita-19, Nishi-8, Kita-ku, Sapporo, Hokkaido 060-0819, Japan

³Department of Electrical Engineering, Graduate School of Engineering, Osaka University, 2-1 Yamadaoka, Suita, Osaka 565-0871, Japan

⁴Japan Aerospace Exploration Agency (JAXA), 2-1-1 Sengen, Tsukuba, Ibaraki 305-8505, Japan

⁵Advanced Engineering Services Co., Ltd., Tsukuba Mitsui Bldg., 1-6-1 Takezono, Tsukuba, Ibaraki 305-0032, Japan

⁶Graduate School of Natural Sciences, Nagoya City University, 1 Yamamahata, Mizuho-cho, Mizuho-ku, Nagoya, Aichi 467-8501, Japan

⁷Japan Space Forum, 3-2-1 Surugadai, Chiyoda, Tokyo 101-0062, Japan

⁸Olympus Optical Co., Hachioji, Tokyo 192-8507, Japan

(Received 23 October 2015; accepted 15 February 2016; published online 15 March 2016)

To clarify the growth mechanism of a protein crystal, it is essential to measure its growth rate with respect to the supersaturation. We developed a compartment (growth cell) for measuring the growth rate ($<0.1 \text{ nm s}^{-1}$) of the face of a protein crystal at a controlled supersaturation by interferometry over a period of half a year in space. The growth cell mainly consists of quartz glass, in which the growth solution and a seed crystal are enclosed by capillaries, the screw sample holder, and a helical insert. To avoid the destruction of the cell and the evaporation of the water from the solution inside the cell, we selected the materials for these components with care. The equipment was successfully used to examine the growth of a lysozyme crystal at a controlled supersaturation in space, where convection is negligible because of the microgravity environment, thereby advancing our understanding of the mechanism of protein crystal growth from solution. The technique used to develop the growth cell is useful not only for space experiments but also for kinetic studies of materials with very slow growth and dissolution rates ($<10^{-3} \text{ nm s}^{-1}$). © 2016 AIP Publishing LLC. [<http://dx.doi.org/10.1063/1.4942961>]

I. INTRODUCTION

The crystallization of proteins from aqueous solution is an experiment that has frequently been performed in space because relatively large and well-ordered protein crystals are successfully generated compared with those grown under terrestrial conditions.^{1,2} Because these traits are advantageous for the X-ray structural analysis of protein molecules, many attempts have been made to obtain high-quality crystals in microgravity environments.^{3–6} To achieve successful crystallization with the limited opportunities available, instruments that can be used in space must be designed to overcome the many inherent restrictions^{7–9} and to generate high-quality protein crystals.

However, when investigating crystal growth mechanisms, it is essential to observe growing crystals and to measure their growth rates under controlled crystallization conditions, including the supersaturation, the concentration, and the temperature. There is a direct relationship between the quality of crystals and their growth history.¹⁰ Consequently, the

growth rates of protein crystals were measured at controlled supersaturation using recoverable satellites or aircraft. In some of these experiments, the growth rates under microgravity were higher than those observed under terrestrial conditions, contrary to the expectation,^{11,12} because common sense suggests that the convection in solution should provide more solute to the growing crystal surface under terrestrial conditions. Why protein crystals formed in space have a higher degree of perfection and a greater growth rate is still not understood. Therefore, we undertook the space experiment project “NanoStep” to clarify this phenomenon and to extend our understanding of ground-based crystallization processes. The protein crystallization experiment of NanoStep had to be performed under conditions of controlled supersaturation. Here, we report the details of the especially designed experimental compartment (growth cell) that was responsible for the success of the experiment in space.

II. THE NANOSTEP PROJECT

A. Overview

The space experiment NanoStep, which investigated the growth of a protein crystal in aqueous solution under

^{a)}Author to whom correspondence should be addressed. Electronic mail: yamazaki@lowtem.hokudai.ac.jp

microgravity conditions, was performed in the Japanese Experimental Module (KIBO) of the International Space Station (ISS) in 2012.¹³ We developed the Experimental Unit (EU) for the observation of protein crystals using the Solution Crystallization Observation Facility (SCOF) onboard KIBO.¹³ The surfaces of the protein crystals were observed and their growth rates were measured by a Michelson-type interferometry¹⁴ in the EU. The concentration field around the crystal was also measured by a Mach–Zehnder-type interferometry¹⁵ equipped with the SCOF. These observations had to be performed in 180 days under conditions of controlled supersaturation σ , defined as $\ln(C/C_e)$, where C is the bulk concentration of the protein and C_e is its solubility. The solubility of our protein sample, hen egg-white lysozyme, depends strongly on the temperature and concentration of the precipitant, NaCl. The supersaturation of the crystallization solutions of proteins used in previous space experiments to produce high-quality crystals was not uniform, because the proteins and precipitants were mixed gradually to produce a broad supersaturation to allow crystallization under microgravity conditions. The growth cells used in those systems were not suitable for our experiment because our observations had to be made under controlled supersaturation. Therefore, we designed a growth cell suitable for our project.

B. Requirements of the growth cell

To measure crystal growth rates under controlled supersaturation on the ground, a seed crystal and its growth solution are sealed in a growth cell^{16,17} or the growth solution is continuously passed through the growth cell at a constant temperature.^{14,18} These growth cells permit the observation of crystal growth at fixed supersaturation by controlling the concentrations of the protein and precipitants and the temperature. We could use such a system in space experiments, but a system for passing the solution into the cell would require a large space for the instruments and would increase the risk of failure because of the great complexity of the instrumentation. Therefore, we designed a closed cell with a seed crystal and growth solution at the given protein and precipitant concentrations, and we observed the crystal growth at various supersaturation by controlling the overall temperature of the growth cell.

For the purposes of the NanoStep project, the closed growth cell had to satisfy several optical and mechanical requirements. The growth cell had to permit the observation of the crystal, the measurement of growth rates as small as 0.1 nm s^{-1} from the crystal surface, and the determination of the concentration field around the crystal by applying the techniques of interferometry. Because the formation of suitable fringes for each measurement was necessary, several devices were required to design the growth cell. Because our project was conducted in an isolated environment over a long period, it was necessary to avoid the destruction of the growth cell or the evaporation of the growth solution, which would have ruined the experiment. Supersaturation was controlled by changing the temperature within the range of $10\text{--}40^\circ\text{C}$ for fixed concentrations of lysozyme and NaCl. Consequently,

the closed cell had to withstand the stresses caused by the thermal expansion of the growth solution and of the materials that composed the cell. Evaporation of the growth solution would change its concentration. In particular, changes in the NaCl concentration would be especially important because the solubility of lysozyme is strongly dependent on this concentration.¹⁹ High levels of evaporation of the growth solution might increase the NaCl concentration, significantly reducing the solubility of the lysozyme. At the start of the experiment, all crystals except the cross-linked seed crystal²⁰ had to be dissolved completely by increasing the temperature.¹³ If the solubility of lysozyme at 40°C , the upper limit of our temperature-controlled range, became less than the initial lysozyme concentration, the crystals would not dissolve completely, complicating the calculation of the degree of supersaturation and resulting in the formation of undesired crystals, as well as generating bubbles in the cell.

III. THE GROWTH CELL

A photograph of the growth cell and a schematic representation of it are shown in Figs. 1(a) and 1(b), respectively. The body of the cell was made of quartz glass, which has good chemical resistance and transmits visible light, allowing interferometric observations. Two quartz glass capillaries were attached to the body with ultraviolet-curing resin as the adhesive to permit the exchange of the growth solution. Each capillary was sealed with an elastomer tube that was closed by wires after the cell had been filled with growth solution. To allow the insertion of a seed crystal into the growth cell, the sample module, consisting of a screw sample holder, a helical insert, and a greased O-ring, was attached to the cell body with ultraviolet-curing resin (Fig. 1(c)). Two reference mirrors were glued to the tip of the screw sample holder, together with a seed crystal, to allow the precise measurement of the growth rates.

The details of the various parts of the growth cell (the cell body, sample module, and tube) are described below.

A. Cell body

The main part of the cell body consisted of quartz glass with outer dimensions of $15 \times 15 \times 9 \text{ mm}$. The thickness of the region of the cell body that formed the laser-light path had to be uniform and free of distortion to permit the appropriate formation of the interferometric fringes. These fringes contained information on the growth rates of the crystal and the concentration field around the crystal as a result of the changes in the optical path length. Therefore, any factors that disturbed the formation of the fringes had to be avoided.

The cell body had to be maintained at an even temperature, because any nonuniformity in the temperature of the cell body would have distorted the glass and thus caused the deformation of the interference fringes, and could also have caused imprecise measurements of the crystal growth rates. The temperature of the cell body was controlled by thermal conduction from copper blocks, the temperature of which was regulated by Peltier elements. Uniform contact between the

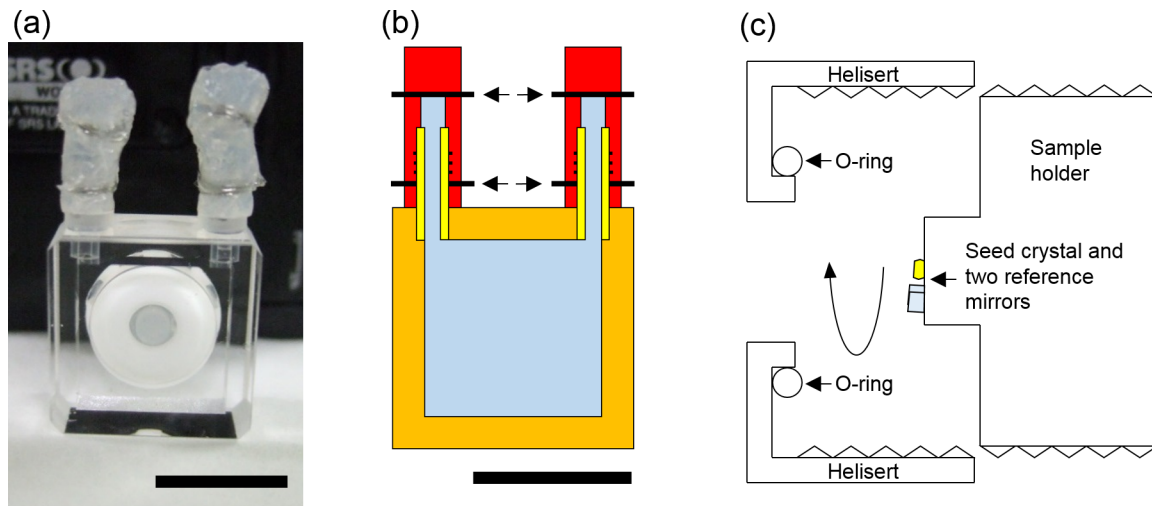


FIG. 1. (a) An example of the growth cell that we fabricated for the space experiment. The white ring is a ceramic helical insert on which the screw sample holder, made of a resin with low water absorptivity, is placed. The scale bar is 10 mm. (b) Schematic illustration of the growth cell without the ceramic helical insert. The body of the growth cell is made of quartz glass (orange). Two capillaries of quartz glass with rubber stoppers (yellow) are fixed to the body with an adhesive. Tubes of elastomer (red) are attached to each capillary. After the growth cell is filled with the growth solution (light blue), the tubes are closed with metal wires (indicated by arrows). The scale bar is 10 mm. (c) A schematic illustration of the helical insert, O-ring, and sample holder with a seed crystal and the reference mirrors.

cell body and the copper blocks ensured an even temperature. Spring screws, which were important for preventing the destruction of the growth cell during the thermal expansion of the blocks and the cell, were used to sandwich the two copper blocks to the cell body with even pressure.¹³ To check the stability of the temperature of the growth cell, we maintained it between 21 and 18 °C, which was measured with a thermocouple attached to the copper block, and continuously observed the interference fringes on the reference mirror (Fig. 2(a)). The interference fringes on the reference mirror

moved in response to the thermal contractions of the growth cell, reference mirrors, solution, and copper blocks induced by temperature changes (Fig. 2(b)). However, 600 s after the temperature was set to 18 °C, the fringes stopped moving, and stayed in the same position, indicating that the temperature of the whole system was uniform and stable. Moreover, the angles of the fringes on the reference mirrors were almost the same at 0 s and 2400 s ($\sim 4^\circ$ from horizontal) and the number of fringes remained unchanged (Fig. 2(c)). These observations showed that no thermally induced stress variations occurred

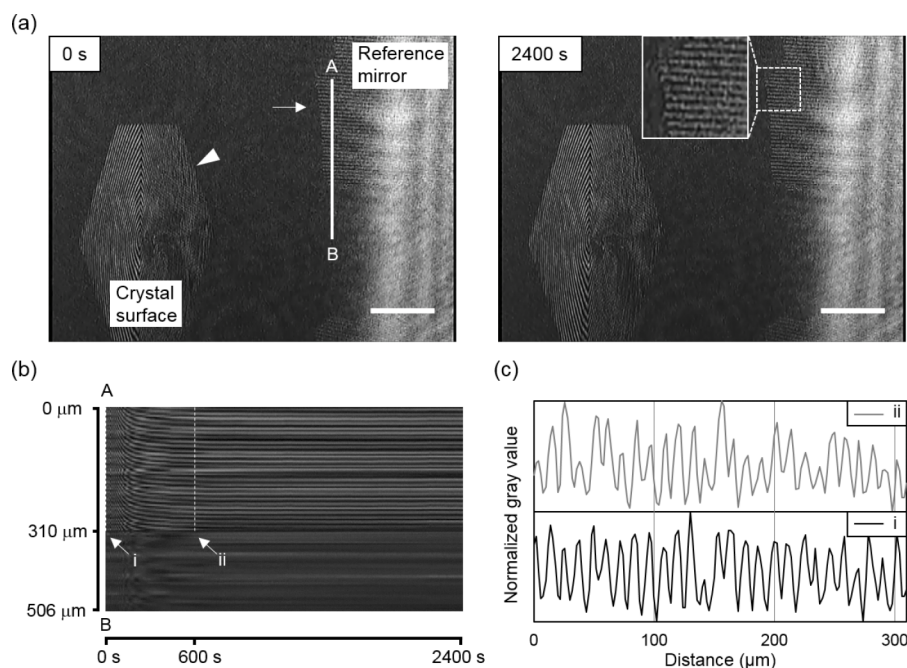


FIG. 2. (a) Interferograms of the lysozyme crystal surface (indicated by a triangle) and reference mirror (indicated by an arrow). The bright part to the right of each image is the reflection from the glass surface. Temperature was set to 21–18 °C at 0 s, and the movement of the fringes on the reference mirror was observed continuously for 2400 s. A part of the interference fringes on the reference mirror at 2400 s are partly enlarged (surrounded by the dashed line). The scale bar is 200 μm . (b) Stacked image of the A–B line in (a) from 0 s (the point at which the temperature began to change) to 2400 s. (c) Normalized gray values for the interferograms at 0 s and 600 s indicated by the dashed lines i and ii in (b), respectively. The top and bottom peaks indicate the positions of the bright and dark lines of the fringes, respectively. The numbers of bright lines for i and ii are the same (= 27).

over the limited temperature difference of 3 °C, between 18 and 21 °C.

The possibility of the destruction of the growth cell can be roughly estimated from the stress arising from the thermal expansion of the growth solution inside it. Suppose the growth cell is a rectangular quartz glass box with internal dimensions of 11 × 11 × 3 mm, and the inside of this box is filled with growth solution. We used lysozyme as the protein sample for the NanoStep and introduced it into the growth cell at 20 °C. We subsequently altered the temperature of the growth cell to a maximum of 40 °C or a difference in temperature of 20 K. This temperature change increased the volume of the lysozyme solution by $dV/V \approx 0.0035$.²¹ The stress on the growth cell resulting from the thermal expansion of the growth solution, σ_q , can be calculated with Hooke's law as follows:

$$\sigma_q = \frac{dV}{V} E_q = 252 \text{ MPa}, \quad (1)$$

where E_q is the Young's modulus of quartz glass (~72 000 MPa). Therefore, the stress on the growth cell exceeded the ultimate tensile strength of the quartz glass (~48 MPa), so the growth cell would be fractured by this temperature change. To prevent the destruction of the quartz glass by accommodating the stresses produced by the thermal expansion of the growth solution, we attached soft elastomer tubes to the growth cell (the selection of the soft elastomer tubing is discussed in Section III C). Because the Young's modulus of the elastomer was <110 MPa,²² lower than that of quartz glass, the stress produced by the thermal expansion of the growth solution was buffered by the distortion of the elastomer tubes.

B. Sample module

To measure the growth rates with Michelson-type interferometry, the detection of the light reflected from the surface of a lysozyme crystal is essential for the appropriate formation of the interference fringes. However, the intensity of the reflected light from the surface of a lysozyme crystal is weaker than that from the growth cell (Fig. 2(a)). Therefore, if these two reflected lights enter the detector at the same position, the intensity of the fringes will be distorted by the reflections from the glass surfaces of the growth cell. To avoid the detection of this light reflected from the growth cell, both the seed crystal and reference mirrors were oriented on the sample holder in a direction tilted by approximately 3° from the surface of the growth cell.¹³ With this arrangement, it was possible to detect the reflections from the crystal surface and reference mirrors exclusively. Another method for eliminating the light reflected from the growth cell is to set a pinhole at an appropriate position in the optical path. However, we did not use this method because if the position of the pinhole was to move slightly during launch, observation would be impossible because the pinhole would obstruct the reflected light from the surface of the crystal. Therefore, we selected the former method to eliminate the reflected light from the growth cell. The principal difficulty with this method is the arrangement of the angle of the seed crystal. The sample holder with a seed crystal and reference mirrors must be selected carefully to ensure good interferometric measurements. Our sample

module permitted the sample holder to be changed easily, so that the appropriate samples for interferometry could be selected from a number of sample holders used with one glass cell body on the ground.

The helical insert, which contacts the quartz glass, was manufactured from ceramic material with extremely low thermal expansivity and water absorptivity, because these factors would otherwise directly induce stress in the quartz glass. The ceramic also had sufficient compressive strength to withstand stress from the glass cell body. In long-term experiments, the possibility of water absorption cannot be neglected. In an initial trial, a helical insert made from a resin that was inexpensive, easily processed, and with sufficient compressive strength was tested for use in the growth cell. When the growth solution had been enclosed in the growth cell for 1 month, the growth cell was destroyed, even though it had been maintained at a constant temperature of 24–25 °C (Fig. 3). After 1 month, the diameter of the resin helical insert had expanded by about 2%. Therefore, we concluded that the destruction of the cell was caused by the expansion of the helical insert as a result of its absorption of water.

The laser can be reflected from the surface of the sample holder just behind the seed crystal and the reference mirrors if the surface is rough. Such unexpected reflections will disturb the interferogram from the crystal and reference mirrors. To avoid these reflections, we made the surface as smooth as possible and confirmed that the interferogram from the crystal and the reference mirrors was not disturbed during interferometry (Fig. 2(a)). We also chose a resin that transmitted as much light as possible.

To prevent the leakage of the solution between the sample holder and the helical insert, we used a greased silicone rubber (SR) O-ring that was soft and showed good chemical resistance to our growth solution. However, we found that air bubbles formed around the sample holder after the construction of the growth cell (Fig. 4). The air bubbles formed between the sample holder and the helical insert, and their shapes were distorted by these two bodies. From their shapes, the bubbles appeared to have formed and subsequently grown *in situ*. The source of the air bubbles might have been the O-ring, because silicone rubber often absorbs air. Therefore, we soaked the O-ring in the growth solution before assembly to prevent the formation of air bubbles in the growth cell.

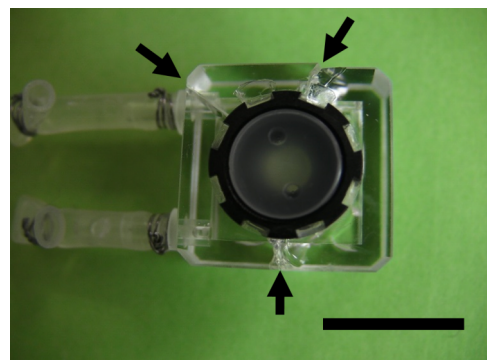


FIG. 3. A photograph of the destroyed trial growth cell. This growth cell has a black resin helical insert. The arrows show the cracks in the cell body. The scale bar is 10 mm.

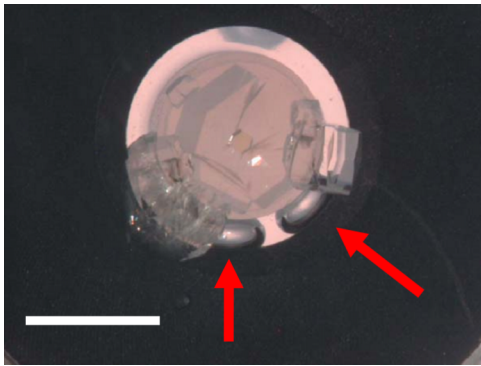


FIG. 4. A photograph of the air bubbles formed in the sample module. The arrows show the air bubbles trapped between the sample holder and the helical insert. The scale bar is 2 mm.

Two reference mirrors on the sample holder were used to correct the growth rates. Fringes can fluctuate as a result of mechanical shaking, the movement of air, or changes in the temperature of the instrument as a whole. Therefore, the movement of the fringes on the crystal surface required correction with reference mirrors.²³ The use of two reference mirrors also permitted the detection of distortions in rotation. Therefore, after fabricating the growth cell, we ensured that the growth cell caused no distortion by observing the fringe movements formed on the two reference mirrors.

C. Tube

Our growth cell had to be attached to soft elastomer tubes to prevent its destruction during the thermal expansion of the growth solution, as described in Section III A. However, elastomers such as silicone rubber are often permeable to gases or solvents, which would have caused the evaporation of the growth solution. To maintain constant concentrations of proteins and precipitants inside the cell in the NanoStep, it was necessary to prevent the evaporation of water from the cell for >180 days to ensure that the measurements were obtained under constant conditions. Therefore, we selected a suitable elastomer that would prevent the evaporation of the growth solution. To do so, we evaluated the evaporation of water through four types of elastomer tubes: poly(vinyl chloride) (PVC), silicone rubber (SR), polyolefin-coated SR (OC-SR), and low-moisture-permeability thermoplastic elastomer (LMP-TPE). The inner diameter (I.D.), outer diameter (O.D.), and durometer hardness of the PVC, SR, and LMP-TPE tubes are listed in Table I. OC-SR is manufactured by coating an SR tube with an olefin-based sealant, which is cured at 100 °C

TABLE I. I.D., O.D., and Shore A durometer hardness at 15 s for the PVC, SR, and LMP-TPE tubes.

Elastomer	I.D. (mm)	O.D. (mm)	Shore A durometer hardness (15 s)
PVC	1.6	3.2	55
SR	1.6	3.2	50
LMP-TPE	1.5	3.2	62



FIG. 5. An example of the sample tubing used to measure the rate of evaporation of water. The tube was filled with double-distilled water. The sample shown is LMP-TPE tubing. The scale bar is 10 mm.

for 30 min. Consequently such a polyolefin coating cannot be applied to materials with low thermal resistance, such as PVC. We placed double-distilled water into the tubes, sealed them with wire (Fig. 5), and then measured the temporal changes in weight at 20 and 40 °C using a balance (CP225D, Sartorius). From the temporal dependence of the change in weight of each 1 mm tube, we calculated the amount of water that evaporated from within them (Fig. 6). The rate of evaporation of water from the SR tube was fastest among the four types of tube at both 20 and 40 °C. Coating the SR with polyolefin reduced the evaporation rate to a value similar to that of the PVC tube. The lowest rate of evaporation was observed from the LMP-TPE tube. We calculated the evaporation rates from the 1 mm segments of the tubes from the slopes of the linear functions in Fig. 6 (Table II).

We next estimated the amount of evaporation of growth solution that would occur from the tubes in the growth cell in 180 days. Based on the design of the growth cell shown in Fig. 1, we assumed that the amount of growth solution in the growth cell was 381 μL and that the growth solution would evaporate from a 4 mm section of tube.

For the SR tube, about 30% of the growth solution would evaporate at 20 °C and all the solution would evaporate at 40 °C in 180 days. For the PVC and OC-SR tubes, about 4% of the growth solution would evaporate at 20 °C and more than 30% would evaporate at 40 °C. For the purposes of our project, we needed to maintain the temperature at 40 °C for 20% of the experimental period to ensure the complete dissolution of the lysozyme crystals without a chemically cross-linked seed crystal inside the growth cell. Therefore, we estimated that more than 9% of the growth solution would evaporate during the experimental period with these elastomer tubes. In contrast, the LMP-TPE tube strongly suppressed evaporation, and only 0.05% and \sim 1% of the growth solution would evaporate at 20 and 40 °C, respectively. In planning the space experiment, the growth cell was assumed to remain at 40 °C for 20% of the whole experimental period (180 days) and at 20 °C for the rest of the time. Using the evaporation rates for the LMP-TPE tube, the total amount of evaporation of the growth solution during the experimental period would be \sim 1 μL , which is equivalent to \sim 0.3% of the total amount in the growth cell. Therefore, we selected LMP-TPE tubes for the fabrication of the growth cell.

IV. APPLICATION OF OUR GROWTH CELL

Three growth cells of our design have been used in the NanoStep project. During the project, none of the three

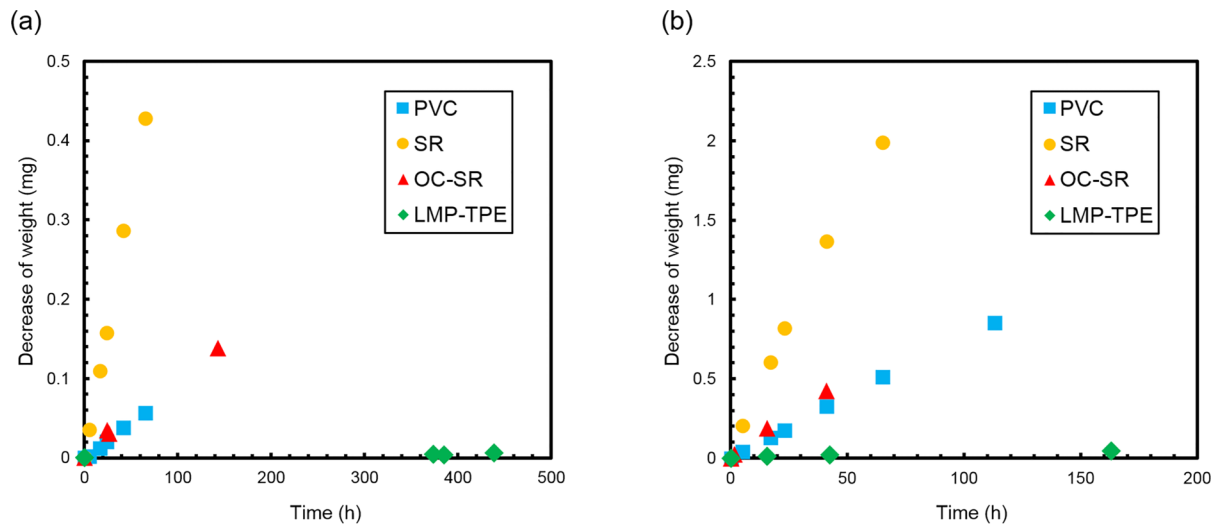


FIG. 6. Rates of weight loss per millimeter of sample tube at (a) 20 °C and (b) 40 °C. The volume of water in each 1 mm of tube was about 2 mg.

growth cells was destroyed, and the growth rates of the crystal surfaces and the concentration fields around the crystals were successfully measured.²⁴ Negligible evaporation of the growth solution was observed in one of three growth cells that had been used in an earlier stage of the NanoStep project. However, slight evaporation of the growth solution was observed in two of the growth cells. One of these cells, which had been used in the last experiment, allowed 2.8% evaporation of water,²⁵ an amount slightly larger than our estimated value. This evaporation may have occurred through the ultraviolet-curing resin used to glue the helical insert and the capillary to the glass. Although the gaps between these were narrow ($\sim 10 \mu\text{m}$), they cannot be ignored in long-term experiments. This resin is useful for filling such narrow gaps without trapping air because its viscosity before curing is low. To improve the growth cell, a glue of low viscosity and extremely low water absorptivity must be developed. However, because the amount of evaporation of water was small and was within the correctable range, the conditions of the growth solution were successfully reconstructed, and precise growth rates at fixed supersaturations were successfully obtained.²⁵ Therefore, we accomplished our aims in the space experiment in the ISS.

Our technique to maintain the growth solution at a constant concentration for long periods is not only useful for the space experiment in the ISS but also, for example, for studying the kinetics of minerals in natural environments. In geological environments, some minerals that are important

for the underground sequestration of carbon dioxide²⁶ or in understanding mineral formation mechanisms²⁷ often have very slow growth and dissolution rates, below $10^{-3} \text{ nm s}^{-1}$. For the precise measurements of such slow rates, it is necessary to keep the growth conditions constant for at least several days. Our technique may also be useful in investigating the kinetics of such minerals.

V. CONCLUSIONS

We developed a growth cell fabricated mainly from quartz glass to observe the growth process of a protein crystal by interferometry in the ISS in a wide temperature range, 10–40 °C. With the careful selection of materials, the growth cell was capable of withstanding the stresses generated by the water absorption and thermal expansion of the growth solution during a temperature change of 20 °C. The growth cell also ensured that the maximum level of evaporation of water from inside the cell was 2.8% during the 180-day experiment. This growth cell will be useful for longer-term experiments involving aqueous solutions in isolated environments, particularly in space experiments.

ACKNOWLEDGMENTS

This work was supported by JAXA for NanoStep project (P. I. K. Tsukamoto). It was also supported by a Grant-in-Aid for Research Activity Start-up from KAKENHI (No. 26887001). It was also supported, in part, by the Tohoku University GCOE program for “Global Education and Research Center for Earth and Planetary Dynamics.” The authors would like to thank Mr. Michael Sakuragi and Saint-Gobain K. K., for their technical support in the selection of the elastomer tubes.

TABLE II. Rates of evaporation of water from each elastomer tube at 20 and 40 °C. These values were calculated from the linear function for the rate of reduction in weight under the relevant conditions, as shown Fig. 5.

Elastomer	Evaporation rate ($\text{g mm}^{-1} \text{ h}^{-1}$)	
	At 20 °C	At 40 °C
PVC	$(9.1 \pm 0.3) \times 10^{-7}$	$(7.6 \pm 0.1) \times 10^{-6}$
SR	$(6.7 \pm 0.1) \times 10^{-6}$	$(3.1 \pm 0.1) \times 10^{-5}$
OC-SR	$(9.4 \pm 0.6) \times 10^{-7}$	$(1.0 \pm 0.1) \times 10^{-5}$
LMP-TPE	$(1.2 \pm 0.3) \times 10^{-8}$	$(2.5 \pm 0.3) \times 10^{-7}$

¹W. Littke and C. John, *Science* **225**, 203 (1984).

²L. J. DeLucas, C. D. Smith, H. W. Smith, S. Vijay-Kumar, S. E. Senadhi *et al.*, *Science* **246**, 651 (1989).

³J. Day and A. McPherson, *Protein Sci.* **1**, 1254 (1992).

⁴J. D. Ng, B. Lorber, R. Giegé, S. Koszelak, J. Day, A. Greenwood, and A. McPherson, *Acta Crystallogr., Sect. D: Biol. Crystallogr.* **53**, 724 (1997).

- ⁵K. Inaka, S. Takahashi, K. Aritake, T. Tsurumura, N. Furubayashi *et al.*, *Cryst. Growth Des.* **11**, 2107 (2011).
- ⁶H. Nakano, A. Hosokawa, R. Tagawa, K. Inaka, K. Ohta *et al.*, *Acta Crystallogr., Sect. F: Struct. Biol. Cryst. Commun.* **68**, 757 (2012).
- ⁷L. J. DeLucas, F. L. Suddath, R. Snyder, R. Naumann, M. B. Broom *et al.*, *J. Cryst. Growth* **76**, 681 (1986).
- ⁸L. A. Gonzalez-Ramirez, J. Carrera, J. A. Gavira, E. Melero-Garcia, and J. M. Garcia-Ruiz, *Cryst. Growth Des.* **8**, 4324 (2008).
- ⁹J. M. Garcia-Ruiz and A. Moreno, *Acta Crystallogr., Sect. D: Biol. Crystallogr.* **50**, 484 (1994).
- ¹⁰I. Yoshizaki, T. Sato, N. Igarashi, M. Natsuisaka, N. Tanaka *et al.*, *Acta Crystallogr., Sect. D: Biol. Crystallogr.* **57**, 1621 (2001).
- ¹¹K. Tsukamoto, G. Sazaki, K. Kojima, M. Tachibana, and I. Yoshizaki, *Space Util. Res.* **25** (2009), <https://repository.exst.jaxa.jp/dspace/handle/a-is/16518>.
- ¹²W. Pan, J. Xu, K. Tsukamoto, M. Koizumi, T. Yamazaki *et al.*, *J. Cryst. Growth* **377**, 43 (2013).
- ¹³I. Yoshizaki, K. Tsukamoto, T. Yamazaki, K. Murayama, K. Oshi *et al.*, *Rev. Sci. Instrum.* **84**, 103707 (2013).
- ¹⁴K. Maiwa, K. Tsukamoto, and I. Sunagawa, *J. Cryst. Growth* **102**, 43 (1990).
- ¹⁵K. Murayama, K. Tsukamoto, A. Srivastava, H. Miura, E. Yokoyama *et al.*, *Cryst. Res. Technol.* **49**, 315 (2014).
- ¹⁶P. Dold, E. Ono, K. Tsukamoto, and G. Sazaki, *J. Cryst. Growth* **293**, 102 (2006).
- ¹⁷A. E. S. Van Driessche, G. Sazaki, F. Otálora, F. M. González-Rico, P. Dold *et al.*, *Cryst. Growth Des.* **7**, 1980 (2007).
- ¹⁸M. Maruyama, K. Tsukamoto, G. Sazaki, Y. Nishimura, and P. G. Vekilov, *Cryst. Growth Des.* **9**, 127 (2009).
- ¹⁹E. Cacioppo and M. L. Pusey, *J. Cryst. Growth* **114**, 286 (1994).
- ²⁰Y. Iimura, I. Yoshizaki, L. Rong, S. Adachi, S. Yoda *et al.*, *J. Cryst. Growth* **275**, 554 (2005).
- ²¹W. J. Fredericks, M. C. Hammonds, S. B. Howard, and F. Rosenberger, *J. Cryst. Growth* **141**, 183 (1994).
- ²²M. F. Ashby, *Acta Metall.* **37**, 1273 (1989).
- ²³H. Satoh, Y. Nishimura, K. Tsukamoto, A. Ueda, K. Kato *et al.*, *Am. Mineral.* **92**, 503 (2007).
- ²⁴Y. Suzuki, K. Tsukamoto, I. Yoshizaki, H. Miura, and T. Fujiwara, *Cryst. Growth Des.* **15**, 4787 (2015).
- ²⁵T. Fujiwara, Y. Suzuki, I. Yoshizaki, K. Tsukamoto, K. Murayama *et al.*, *Rev. Sci. Instrum.* **86**, 083704 (2015).
- ²⁶M. Sorai, T. Ohsumi, M. Ishikawa, and K. Tsukamoto, *Appl. Geochem.* **22**, 2795 (2007).
- ²⁷A. E. S. Van Driessche, J. M. Garcia-Ruiz, K. Tsukamoto, L. D. Patino-Lopez *et al.*, *Proc. Natl. Acad. Sci. U. S. A.* **108**, 15721 (2011).